Molecular Therapy
Original Article

A Targeted and Stable Polymeric Nanoformulation Enhances Systemic Delivery of mRNA to Tumors

Qixian Chen,[1,2,7] Ruogu Qi,[3,7] Xiyi Chen,[4] Xi Yang,[5] Sudong Wu,[6] Haihua Xiao,[3] and Wenfei Dong[1]

[1]CAS Key Laboratory of Bio-Medical Diagnostics, Suzhou Institute of Biomedical Engineering, Suzhou 215163, China; [2]Department of Chemistry, Massachusetts Institute of Technology, Cambridge, MA 02139, USA; [3]State Key Laboratory of Polymer Physics and Chemistry, Changchun Institute of Applied Chemistry, Chinese Academy of Sciences, Changchun 130022, China; [4]School of Public Health, Dalian Medical University, No. 9 West Section Lvshun South Road, Dalian 116044, China; [5]Department of Neurosurgery, Renji Hospital, Shanghai Jiao Tong University School of Medicine, Shanghai 200127, China; [6]Ningbo Institute of Material Technology and Engineering, Chinese Academy of Sciences, Ningbo 315201, China

The high vulnerability of mRNA necessitates the manufacture of delivery vehicles to afford adequate protection in the biological milieu. Here, mRNA was complexed with a mixture of cRGD-poly(ethylene glycol) (PEG)-polylysine (PLys) (thiol) and poly(*N*-isopropylacrylamide) (PNIPAM)-PLys(thiol). The ionic complex core consisting of opposite-charged PLys and mRNA was crosslinked though redox-responsive disulfide linkage, thereby avoiding structural disassembly for exposure of mRNA to harsh biological environments. Furthermore, PNIPAM contributed to prolonged survival in systemic circulation by presenting a spatial barrier in impeding accessibility of nucleases, e.g., RNase, due to the thermo-responsive hydrophilic-hydrophobic transition behavior upon incubation at physiological temperature enabling translocation of PNIPAM from shell to intermediate barrier. Ultimately, the cRGD ligand attached to the formulation demonstrated improved tumor accumulation and potent gene expression, as manifested by virtue of facilitated cellular uptake and intracellular trafficking. These results indicate promise for the utility of mRNA as a therapeutic tool for disease treatment.

INTRODUCTION

Gene therapy is rooted in the concept of delivering the therapeutic genomic sequence into the nuclei of the targeted cells, subsequently inducing expression of the encoded functional proteins and exerting therapeutic outcomes.[1–4] Nevertheless, its translation into clinical trial has been restricted primarily due to insufficient activity of transgene expression by the delivery vehicles and the threat of insertional mutagenesis associated with the use of DNA. As an alternate genomic material to DNA, mRNA has been postulated to encompass distinctive advantages, including no requirement for nuclear entry, which poses a significant barrier for DNA delivery vehicles.[5–7] In addition, mRNA is suspected to possess minimal possibility of integrating into the host genome.[8] Therefore, mRNA is encouraging as an alternative method of gene delivery. However, wide realization of mRNA-based therapeutics has been inhibited because of its intrinsically high vulnerability to expressed nucleases.[9] To address these drawbacks, a promising modality of polymeric micelle delivery system, developed for plasmid DNA delivery, was explored for mRNA delivery.[10] The formation of polymeric micelles was based on self-assembly of block catiomers poly(ethylene glycol) (PEG)-polycation (e.g., poly(lysine) [PLys]) and nucleic acids through electrostatic interactions. The polycationic component was capable of neutralizing the negative charge of mRNA and inducing complexation of mRNA into a nanosized structure. Meanwhile, the hydrophilic PEG component in the diblock copolymer acts as surface coating along the mRNA/polycation complex core. This PEGylation process has been demonstrated to be important to reduce non-specific interactions with biological species, accounting for improved biocompatibility in the biological condition.[11] Nevertheless, the inherent susceptibility of mRNA to nuclease degradation was not sufficiently attenuated by PEGylation alone. Formation of a PEG shell by electrostatic complexation alone was shown to be inadequate to induce sufficient PEG crowding and eliminate accessibility of nanometer-scaled biological compounds, such as RNase.[12] These drawbacks precipitated further development of polymeric micelle system for protecting mRNA in the blood milieu. In the current study, thiol groups were introduced into the cationic PLys segments with the aim of redox-responsive crosslinking the PLys/mRNA complex core to prevent premature structural disassembly of the complex and exposure of the mRNA payload in the harsh biological environment. To reduce the transport of nucleases potentially translocating the PEG shell and causing mRNA degradation, we engineered an appreciable multi-layered polymeric nanostructure, characterized with the aforementioned crosslinked mRNA reservoir spatially protected by sequential hydrophobic barrier and hydrophilic shell (Figure 1). This intriguing architecture was hypothesized to reduce the accessibility of biological components

Received 25 May 2016; accepted 31 October 2016;
http://dx.doi.org/10.1016/j.ymthe.2016.10.006.

[7]These authors contributed equally to this work.

Correspondence: Qixian Chen, Department of Chemistry, Massachusetts Institute of Technology, Cambridge, MA 02139, USA.
E-mail: qixian@mit.edu
Correspondence: Xiyi Chen, School of Public Health, Dalian Medical University, No. 9 West Section Lvshun South Road, Dalian 116044, China.
E-mail: xychen@dmu.edu.cn
Correspondence: Wenfei Dong, CAS Key Laboratory of Bio-Medical Diagnostics, Suzhou Institute of Biomedical Engineering, Suzhou 215163, China.
E-mail: weifeidong@126.com

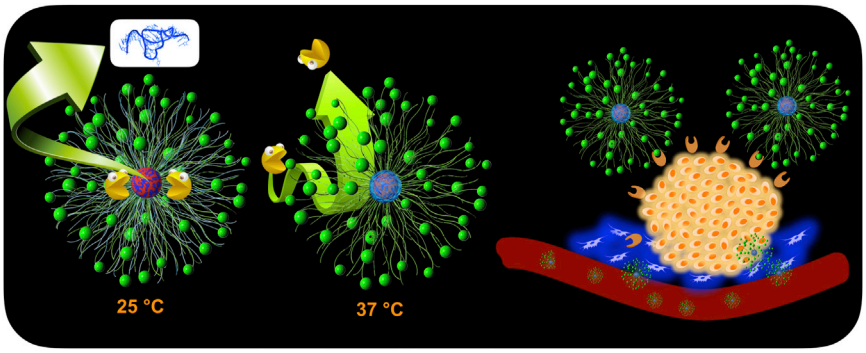

Figure 1. Conceptual Illustration of Polymeric Nanoformulation as an mRNA Delivery System
mRNA (core blue) was electrostatically complexed with PLys (core red) as the complex core, followed by crosslinking through redox disulfide linkage. The thermoresponsive PNIPAM (aqua blue) translocates from shell to collapse onto the complex core as protective intermediate barrier. The external PEG (green chain) is presented as the biocompatible shell. cRGD (green sphere) as ligand was decorated at the distal end of PEG to exert tumor-targeting function.

to the mRNA payload and attenuate the subsequent degradation of mRNA by nuclease, consequently accounting for prolonged blood retention post intravenous injection. Surface decoration of tumor-targeted ligands onto the constructed formulation was also included in order to target delivery of mRNA to the tumors and prompt internalization into the targeted tumor cells for efficient expression in tumors via a systemic route.

RESULTS AND DISCUSSION

Polymer Synthesis and Characterization

Herein, a class of block copolymers was synthesized according to Schemes S1–S3. In brief, methoxy-(PEG)-NH_2 (12 kDa) was used as starting material to polymerize with the monomer N6-trifluoroacetyl-L-lysine N-carboxyanhydride NCA-Lys(TFA) to yield PLys(TFA) segment (Scheme S1).[5] Furthermore, the protective group of TFA in the synthetic PLys(TFA) segment was removed with treatment of 1N NaOH in methanol to yield the ultimate PEG-PLys. The degree of polymerization (n) of the synthetic PLys segment was determined to be n = 55 according to ^{1}H-NMR measurement (Figure S1). A similar synthetic procedure was followed to synthesize acetal-PEG-PLys (Scheme S2). N-succinimidyl 3-(2-pyridyldithio)-propionate (NHS-SPDP) was introduced into the side chain of PLys segment of acetal-PEG-PLys(PDP) (PDP substitution: ~20%; Figure S3). Ultimately, the acetal groups of the yielded acetal-PEG-PLys(PDP) were acidified to transform into aldehyde for conjugation of cRGDfK (functionalized with cysteine; Figure S3). Prior to polymeric formulation, PDP groups were converted to −SH groups under treatment of DTT. The cRGD conjugation efficiency was determined to be 95% according to ^{1}H-NMR measurement (Figure S4).

Poly(N-isopropylacrylamide) (PNIPAM)-PLys(SH) was prepared by following a similar synthetic route, where PNIPAM-NH_2 was used as a macro-initiator for ring-opening polymerization (Scheme S3; ^{1}H-NMR spectrum in Figure S5). For comparison, the control polymers, including PEG-PLys(SH) (^{1}H-NMR spectrum in Figure S2), were also synthesized. The GPC trace of the yielded polymers was characterized by GPC measurement with unimodal molecular weight distribution (Figure S6). The chemical descriptions of diverse polymers were summarized in Table 1.

Preparation and Characterization of Polymeric Nanoformulation

Here, PEG-PLys, PEG-PLys(SH), mixtures of PEG-PLys(SH) and PNIPAM-PLys(SH) (molar ratio of 1:1; referred as PEG/PNIPAM-PLys(SH) hereafter), and mixtures of cRGD-PEG-PLys(SH) and PNIPAM-PLys(SH) (molar ratio of 1:1; referred as cRGD-PEG/PNIPAM-PLys(SH) hereafter) were used to complex with mRNA at an N/P ratio of 1.5, where N/P ratio was defined as the molar ratio of the total primary amine groups of the polymers to the phosphate groups of mRNA. Here, a relatively low N/P ratio of 1.5 (slight overcharge stoichiometry) was selected due to the well-acknowledged free polycation-mediated cytotoxicity. In view of the susceptibility of mRNA in the biological milieu, polymeric micelle based on electrostatic interaction of block copolymer PEG-PLys and mRNA was employed as the platform to accommodate mRNA. The electrostatic reaction between cationic PLys segment and anionic mRNA could lead to formation of complex core whereas the hydrophilic PEG chains tethering at PLys consequently represent the shielding shell surrounding the complex core. Fluid atomic force microscopy (AFM)/transmission electron microscopy (TEM) and dynamic light scattering (DLS) measurement (Figures 2A and S1; Table 2) revealed the resulting PEG-PLys/mRNA complex possessing distinct spherical nanostructures with unimodal distribution (polydispersity index [PDI]: 0.11), ~73 nm in diameter. Numerous literature has validated the crucial role of the existence of PEG shell in reducing the nonspecific interactions with the biological species, e.g., capable of diminishing the structural disassembly caused by exchange interactions with the charged species and lowering the accessibility of the endogenous proteins (thereby committing to reduce enzymatic degradation and protein adsorption-mediated reticuloendothelial system clearance).[12,13] This appreciable platform architecture was further crosslinked by introducing redox-responsive disulfide into the complex core. This strategic crosslinking was postulated to drastically promote the structural stability, thus minimizing the occurrence of direct exposure of the mRNA payload to the harsh biological environment. Pertaining to the exceeding vulnerability of mRNA to the nuclease, an additional intermediate hydrophobic palisade of PNIPAM was proposed on top of the formed PLys interior because a previous report suggests the PEGylation solely driven by electrostatic complexation is not possible to achieve sufficient PEG crowdedness to exclude the accessibility of several nanometer-scaled nucleases. To engineer

Table 1. Chemical Characterization of Diverse Block Polymers

	PEG-PLys	PEG-PLys(SH)	cRGD-PLys(SH)	PNIPAM-PLys(SH)
DP of PLys	55	53	56	55
Thiolation degree (%)	0	20	18	20
cRGD (%)	–	–	95	–
PEG segment (kDa)	12	12	12	–
PNIPAM segment (kDa)	–	–	–	5

DP, polymerization degree.

such intermediate PNIPAM palisade, a mixture of PEG-PLys(PDP) and PNIPAM-PLys(PDP) was complexed with mRNA at 25°C (below lower critical solution temperature of PNIPAM), followed by sequential DTT treatment to retrieve thiol groups (SH) and dialysis in DMSO-containing buffer for disulfide crosslinking at 25°C. Fluid AFM/TEM (Figures 2B and S7) and DLS measurement (Table 2) at 25°C verified a comparable-sized nanoscaled spherical structure to the control polymeric formulation from PEG-PLys, ~73 nm in diameter. Temperature-dependent ^{1}H-NMR measurement was conducted for the aforementioned polymeric formulation of PEG/PNIPAM-PLys(SH) along an increasing gradient to a physiological temperature (37°C), observing progressive decrease in the integrated intensity of PNIPAM relative to PEG. This result suggests the thermo-responsive dehydration of PNIPAM segments aggregate and collapse onto the preformed PLys(SH)/mRNA complex core. In accordance to ^{1}H-NMR measurement, fluid AFM/TEM (Figures 2B and S7) and DLS measurement (Table 2) captured a higher degree of condensed structure, ~58 nm in diameter. A plausible reason for this condensed structure at 37°C should be as a consequence of thermal responsive character of PNIPAM, which induced its hydrophilic-hydrophobic transformation upon thermal gradient to 37°C,[14] consequently accounting for further collapse of PNIPAM onto PLys/mRNA complex, resulting in a thermodynamically stable structure.

Impact of Nanoformulation Architecture on the Survival of mRNA in Biological Milieu

To validate the utility of the aforementioned strategies in improving the survival of mRNA payload in biological milieu, we employed SyBr Green II (immense florescence emission once binds to nucleic acids)[15] as a detecting probe to assess the ability of different formulations in preventing access of biological degradation agents to the mRNA payload. Given that an excess of negatively charged species or structures in the biological milieu potentially enables dissociation of the electrostatic-based formulation,[16] a class of polymeric formulations was incubated with varying concentrations of anionic dextran sulfate in terms of S/P ratio (defined as the molar ratio of the sulfur from dextran sulfate to the phosphate groups from mRNA), followed by addition with SyBr Green II. All polymeric formulations remarkably inhibit the accessibility of SyBr Green II to the encapsulated mRNA payload in absence of dextran sulfate, as evidenced by their

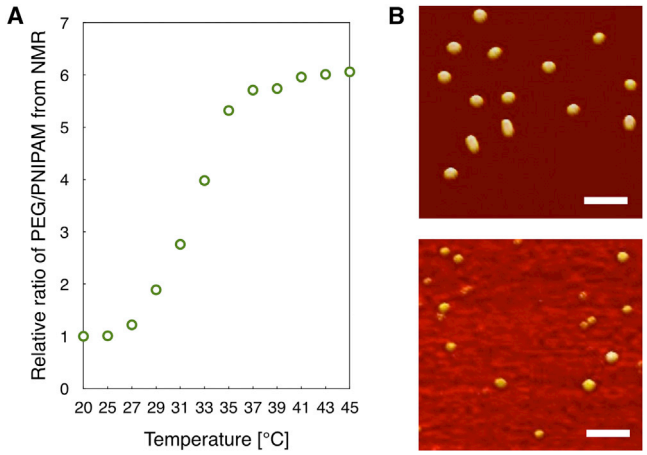

Figure 2. Evaluation of Thermo-responsive Behavior of the Polymeric Nanoformulation

(A) Relative ratio of the integrated area of PEG and PNIPAM from ^{1}H-NMR for the polymeric formulation of PEG/PNIPAM-PLys(SH) at elevated incubation temperature. (B) Fluid AFM characterization of thermo-responsive structural transformation of PEG/PNIPAM-PLys(SH)-based nanoformulations is shown. PEG/PNIPAM-PLys(SH)-based nanoformulations were prepared at 25°C, followed by extended incubation at either 25°C (upper image) or 37°C (lower image).

negligible fluorescence emission in contrast to that of the naked mRNA. Nevertheless, there appeared variable potencies to lowering the accessibility of SyBr Green II to the mRNA payload when incubated with anionic dextran sulfate (Figure 3A). The fluorescence emission of the PEG-PLys formulations was observed to be comparable to that of the naked mRNA at S/P ratio of 10, implying fully structural dissociation of PEG-PLys/mRNA polymeric formulation at high concentration of dextran sulfate. As opposed to the formulation of PEG-PLys/mRNA, disulfide crosslinking could substantially prevent the accessibility of SyBr Green II, despite slight increase in the fluorescence emission detected at high S/P ratios. It was hypothesized that PNIPAM-functionalized formulations under incubation at 37°C, rather than 25°C, could drastically minimize the SyBr Green II fluorescence emission to a background level, affirming the possibility of formation of PNIPAM palisade and its utility in eliminating accessibility of the foreign species to the mRNA payload. Our results suggested the proposed formulation of PEG/PNIPAM-PLys(SH) could serve as an appreciable mRNA delivery vehicle to protect mRNA from degradation in the harsh biological milieu. The subsequent evaluation of mRNA survival in FBS also supported the proposed strategies in protecting mRNA in a biological environment. In these experiments, a class of polymeric formulations containing *Luc* mRNA was incubated in 50% fetal bovine serum (FBS) for 1 hr at 37°C. The remaining intact mRNA was quantified by quantitative real-time PCR measurement (Figure 3B). Apparently, mRNA was subjected to rapid digestion in FBS in PEG-PLys formulation, despite improved survival to some degree as compared to naked mRNA. This result affirmed our speculation that PEGylation alone is inadequate to resolve the enzymatic degradation. On the other hand, complex crosslinking by means of disulfide linkage appeared to

Table 2. Physiochemical Characterization of Polymeric Formulations

	PEG-PLys	PEG-PLys(SH)	PEG/PNIPAM-PLys(SH) 25°C	PEG/PNIPAM-PLys(SH) 37°C	cRGD-PEG/PNIPAM-PLys(SH) 37°C
z-average diameter (nm)	73.1 ± 3.4	72.6 ± 4.2	76.6 ± 3.9	58.1 ± 4.8	58.7 ± 1.7
PDI	0.11 ± 0.02	0.10 ± 0.01	0.09 ± 0.01	0.09 ± 0.02	0.09 ± 0.02
Zeta potential (mV)	2.54 ± 0.29	2.31 ± 0.33	2.21 ± 0.16	2.18 ± 0.34	1.89 ± 0.28

PDI, polydispersity index. The data are expressed as mean ± SD.

remarkably improve the survival of the mRNA payload in FBS, which could be ascribed to disulfide linkage for structural crosslinking so as to minimize the occurrence of structural disassembly against the charged biological species and the possibility of direct exposure of the payload mRNA to the nuclease-rich FBS. Notably, the manufacture of an intermediate hydrophobic palisade from PNIPAM was confirmed to exert a pronounced potency in preventing mRNA from being degraded. Most likely, the presence of hydrophobic palisade behaves as a spatial barrier, lowering the accessibility of nucleases (RNase) to the encapsulated mRNA. These results approved the proposed strategies for improved survival in the biological milieu, thereby its suitability in systemic applications to afford high bioavailability to the targeted site.

Ligand Decoration for Promoted mRNA Expression in Cells

In addition to promoting mRNA survival in the biological milieu, a further strategy was employed to promote systemic targeting efficiency and cellular uptake activity of the established mRNA polymeric formulation. A ligand cyclic Arg-Gly-Asp peptide (cRGD) moiety was attached at the distal end of PEG segment of the block polymer (PEG-PLys(SH)) with the expectation for enhanced cellular uptake by harnessing specific interactions with its receptors ($\alpha_V\beta_3$ and $\alpha_V\beta_5$ integrins) that are overexpressed on the membrane of tumor cells and angiogenic cells.[17–20] To explore the impact of ligand-integrin interaction by cRGD introduction (and the improved mRNA protection by polymeric formulation as well) on the cellular uptake activity, mRNA labeled by fluorescence dye (Cy5) was used to prepare additional polymeric nanoformulations. Cellular uptake efficiency was evaluated in U87 cells (overexpressing $\alpha_V\beta_3$ and $\alpha_V\beta_5$ integrins).[21] Because of the poor survival of PEG-PLys formulation in FBS, the cellular uptake activity was also limited, albeit slightly higher than the background level (Figure 4A). Markedly cellular uptake was obtained for the formulations of PEG-PLys(SH) and PEG/PNIPAM-PLys(SH). This is attributable to the improved survival of mRNA in extracellular and intracellular milieu by means of complex crosslinking and the fabrication of an intermediate PNIPAM barrier, consequently permitting prolonged retention of polymeric formulation in the cellular medium ready for cellular uptake. There was a pronounced increase obtained with cRGD-functionalized formulation (Figure 4A), which could be explained by the improved cell affinity between cRGD-functionalized polymeric formulation and the cell membrane. Consistent with cellular uptake activity, the gene expression efficiency also confirmed the strategies in prolonging the mRNA survival in the biological milieu by disulfide crosslinking and PNIPAM intermediate palisade and increasing cell membrane affinity by cRGD functionalization for pursuit of enhanced gene expression (Figure 4B). On the other hand, pertaining to intracellular distribution, an appreciable low degree of endosome entrapment of cRGD-functionalized formulation (Figures 4C and 4D) was observed, as opposed to non-cRGD formulation, which was consistent with a previous claim that cRGD surface functionalization onto nanoparticles could possibly circumvent digestive endosome entrapment, possibly steering an alternative pathway for intracellular trafficking.[22] Apparently, it is crucially advantageous for mRNA delivery vehicles with regard to the vulnerability of mRNA in the biological milieu.

In Vivo mRNA Expression in Tumors via Intravenous Administration

Ultimately, the nanoformulation of cRGD-PEG/PNIPAM-PLys(SH) was translated in vivo to test its performance as an mRNA delivery vehicle to induce gene expression at the tumor site via a systemic route. Systemic retention, in particular the intactness of mRNA during circulation, post intravenous injection was quantified by quantitative real-time PCR. In our experiments, polymeric nanostructure solutions were administrated intravenously into mice via the tail vein. The blood samples were collected at predefined time intervals and transferred for quantitative real-time PCR analysis. Corroborating in vitro results (i.e., polymeric nanoformulations under FBS incubation), the survival of mRNA in variation formulations exhibited a similar trend, particularly for PNIPAM functionalized formulations (Figure 5A), affirming the use of redox crosslinking and intermediate hydrophobic barrier for improved systemic retention and protection against enzymatic degradation. It should be noted that cRGD-functionalized nanoformulations exhibited prolonged circulation in the bloodstream as compared to non-cRGD formulation, suggesting its utility in systemic applications. To test the efficiency of the proposed system for in vivo expression, we loaded GFP-encoded mRNA into the polymeric nanoformulations, which was intravenously injected to the mice bearing subcutaneous xenografted U87 tumors. At 48 hr postadministration, the tumors were dissected and transferred either for confocal laser scanning microscope (CLSM) observation of GFP expression by cryosection and immunostaining or to homogenize for quantification of GFP expression. Distinct gene expression was observed in tumors (Figures 5C and 5D), especially for the sample of cRGD-PEG/PNIPAM-PLys(SH). Subsequent quantification revealed cRGD-functionalized nanoformulation yielded expression approximately one order of multitude higher than for non-cRGD

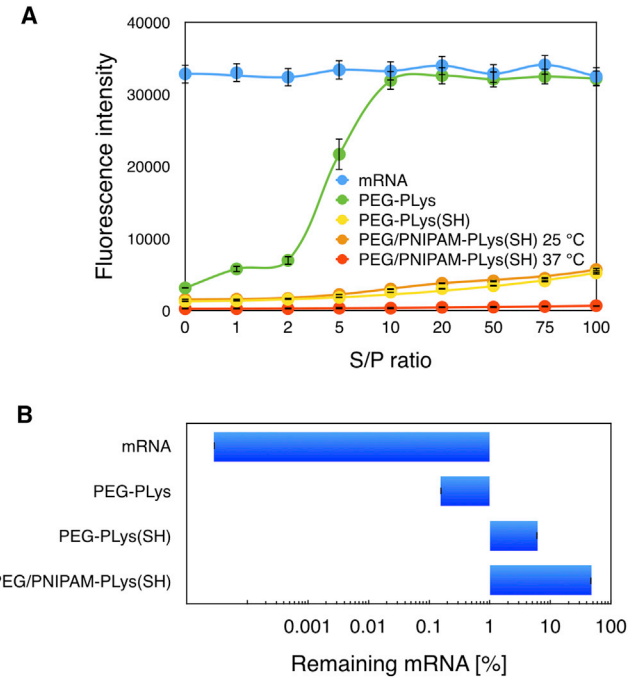

Figure 3. Diverse Polymeric Nanoformulations to Accommodate mRNA Payload for Its Improved Stability in the Biological Milieu

(A) SyBr Green II as a probe to estimate the accessibility of biological species to the mRNA encapsulated in varying formulations as a function of concentration of anionic dextran sulfate. (B) Stability of mRNA encapsulated in varying formulations in presence of FBS is shown (50%; ANOVA analysis was conducted on all the groups; $p < 0.01$).

nanoformulations, which we attributed to improved cell transfection (Figure 4B) and improved tumor-targeted accumulation (Figure 5B). These results validated the strategies of engineering appropriate architecture for protection of the mRNA payload, for persistence in the blood circulation, and for harnessing surface-decorated ligand motifs for enhanced accumulation into the tumor site and subsequent mRNA expression in the targeted tumor cells.

Conclusions

In conclusion, we have developed physicochemical strategies for the formulation of mRNA delivery vehicles capable of targeted delivery and expression of mRNA to the tumors via a systemic route. Incorporation of PNIPAM into the nanoformulation provided an intermediate hydrophobic barrier for reducing the accessibility of nucleases and mitigating associated nuclease degradation. Ligand conjugation to the surface of the polymeric nanoformulation contributed to both improved accumulation at the tumor site and enhanced gene expression of the loaded mRNA via facilitated cellular uptake and intracellular trafficking. Ultimately, the proposed nanoformulation demonstrated enhanced systemic mRNA expression in tumors. These results validate the physicochemical-based approach to engineering for systemic mRNA delivery systems for tumor-targeted gene therapy. The future for mRNA therapeutics is promising.

MATERIALS AND METHODS

Materials

α-methoxy-ω-amino-PEG (PEG) (M_w: 12 kDa) and α-acetal-ω-amino-PEG (acetal-PEG) (M_w: 12 kDa) were purchased from Laysan Bio. Amine-functionalized PNIPAM (M_w: 5 kDa) was purchased from Sigma Aldrich China. Lys(TFA)-NCA was purchased from Carbosynth. Cyclo(RGDfK(C-ε-Acp)) (cRGD) peptide (ε-Acp [6-aminocaproic acid]) was purchased from Peptide Institute. SPDP and slide-a-lyzer dialysis cassettes (molecular weight cut-off [MWCO] = 10 kDa) were purchased from Thermo Scientific. mRNA-encoding reporting sequence of luciferase (*Luc*) was prepared from template pGL4.13 DNA (Promega) by in vitro transcription using the mMESSAGE mMACHINE T7 Ultra Kit (Ambion; Invitrogen), followed by polyadenylation with the poly(A) tail kit (Ambion). mRNA encoding reporting sequence of GFP was purchased from TriLink Biotechnologies. mRNAs were labeled with Cy5 using the Label IT Tracker Intracellular Nucleic Acid Localization Kit obtained from Mirus Bio, according to the manufacturer's protocol. DMEM and Dulbecco's PBS (DPBS) were purchased from Sigma-Aldrich. FBS was purchased from Dainippon Sumitomo Parma. SyBr Green II cell culture lysis buffer and Luciferase Assay System Kit were purchased from Sigma Aldrich China. Rat monoclonal antibody against mouse platelet endothelial cell adhesion molecule-1 (PECAM-1) was purchased from Santa Cruz Biotechnology. Alexa-Fluor-647-conjugated (A21247) goat anti-rat was obtained from Invitrogen Molecular Probes. U87 cells (U-87 MG [American Type Culture Collection HTB-14]) were obtained from the ATCC. BALB/c-nude mice (female; 5 weeks old) were purchased from Charles River Laboratories. All animal experimental procedures were performed in compliance with the Guidelines for Animal Experiment as stated by the Animal Committee of China Academy of Science.

Synthesis of PEG-PLys

Block copolymer PEG-PLys was synthesized according to a ring-opening polymerization approach. In brief, monomer of Lys(TFA)-NCA was polymerized from the initiation of the ω-NH_2 terminal group of MeO-PEG-NH_2 in *N*,*N*-dimethylformamide (DMF). The molecular weight distribution (M_w/M_n) of the yielded PEG-PLys(TFA) was determined to be 1.05 according to a gel permeation chromatography (GPC) equipped with TOSOH HLC-8220 calibrated based on varying M_w of commercial PEG standards. MeO-PEG-PLys(TFA) was dissolved in methanol containing 1 N NaOH with the aim of removing protective TFA groups at 30°C for overnight reaction. The synthetic PLys segment was determined to be 55 based on the peak intensity ratio of the methylene protons of PEG ($(CH_2)_2O$; δ = 3.7 ppm) to the β-, γ-, and δ-methylene protons of lysine ($(CH_2)_3$; δ = 1.3–1.9 ppm) units from the captured ^{1}H-NMR spectra (Figure S1).

Synthesis of Acetal-PEG-PLys

Following a similar synthetic procedure, acetal-PEG-PLys was also synthesized. M_w/M_n of the synthesized acetal-PEG-PLys(TFA) was determined to be 1.06 from GPC. The degree of polymerization (n)

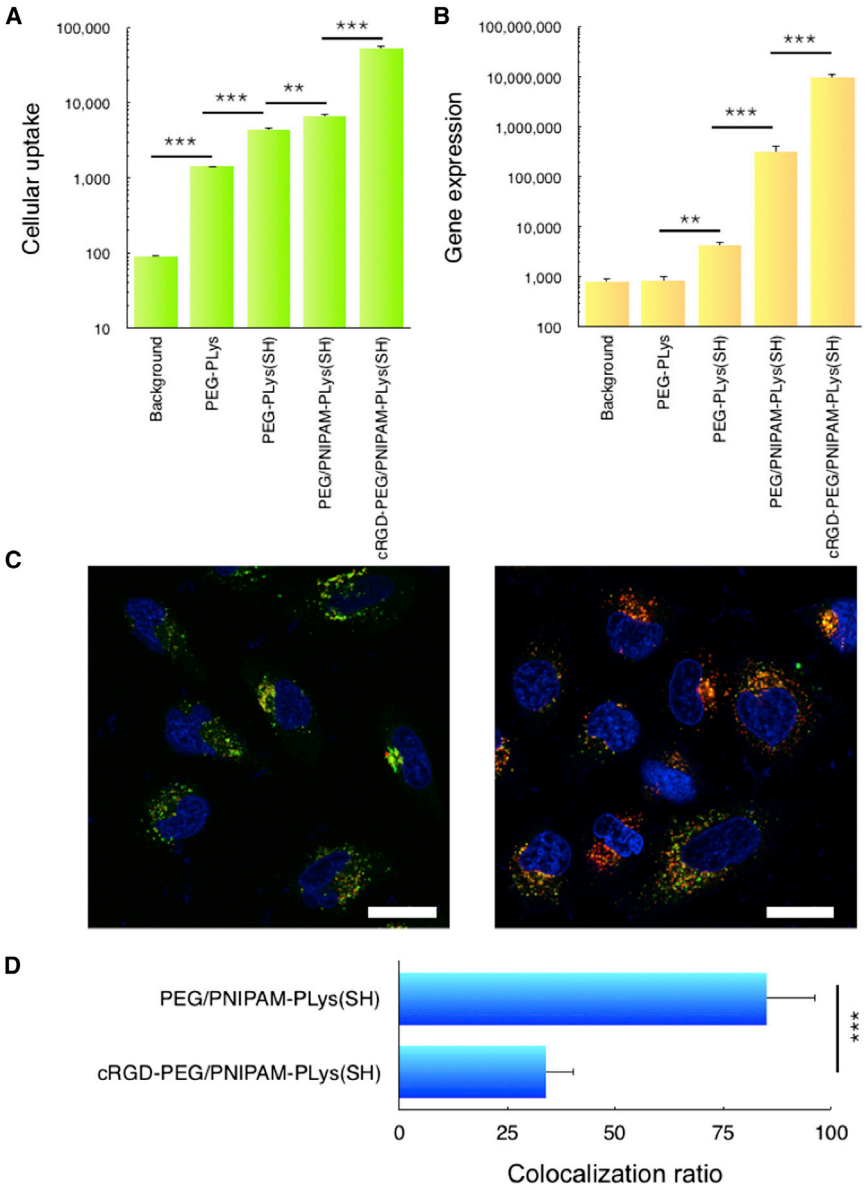

Figure 4. In Vitro Performances of Various Polymeric Nanoformulations in U87 Cells

(A) Cellular uptake; control group represents background level. (B) mRNA expression activity is shown; note that the control group stands for the background level. (C) Intracellular distribution of mRNA by the polymeric nanoformulation of PEG/PNIPAM-PLys(SH) (left) and cRGD-PEG/PNIPAM-PLys(SH) (right) is shown, where cell nuclei was stained into blue, late endosome/lysosome was stained into green, and mRNA was stained into red. (D) Quantified colocalization degree of mRNA and late endosome/lysosome is shown. The scale bar represents 20 μm. *$p < 0.01$; **$p < 0.005$.

of PLys was determined to be (n = 53) according to ^{1}H-NMR measurement.

Synthesis of Thiolated PEG-PLys: PEG-PLys(SH)

Thiolated PEG-PLys(SH) was prepared by introducing pyridyldithiopropionyl (PDP) groups into the side chain of lysine units of the PLys segment of PEG-PLys using the heterobifunctional reagent SPDP. In brief, PEG-PLys was dissolved in *N*-methyl-2-pyrrolidone (NMP) supplemented with 5 wt% LiCl and reacted with predefined concentration of SPDP in anhydrous NMP containing *N*,*N*-diisopropylethylamine (10 mol excess against SPDP) at room temperature. After 4 hr reaction, the crude product was purified by precipitation into diethyl ether. Furthermore, the precipitated product was dissolved in 0.01 N HCl, dialyzed against the distilled water three times, and lyophilized to obtain powder of PEG-PLys(PDP) product. The introduction ratio of thiol groups was determined from the ^{1}H-NMR spectrum recorded in DCl containing D_2O (pD = 2.4) at 25°C by the peak intensity ratio of the β-, γ-, and δ-methylene protons of lysine ($(CH_2)_3$; δ = 1.3–1.9 ppm) to the pyridyl protons of the 3-(2-pyridyldithio) propionyl group (C_5H_4N; δ = 7.2–8.3 ppm). The degree of thiol group substitution was determined to be ∼20% (Figure S2). PEG-PLys(SH) was obtained by treating PEG-PLys(PDP) with DTT.

Synthesis of Thiolated Acetal-PEG-PLys: Acetal-PEG-PLys(SH)

Block polymer acetal-PEG-PLys(PDP) was synthesized according to a similar synthetic procedure, which was further used for cRGD ligand conjugation. The introduction ratio of thiol groups was determined from the ^{1}H-NMR spectrum recorded in DCl containing D_2O (pD = 2.4) at 25°C by the peak intensity ratio of the β-, γ-, and δ-methylene protons of lysine ($(CH_2)_3$; δ = 1.3–1.9 ppm) units to the pyridyl protons of the 3-(2-pyridyldithio) propionyl group (C_5H_4N; δ = 7.2–8.3 ppm). The degree of thiol group substitution was determined to be 18% by referring to the total units of PLys segment (Figure S4). The deprotective form of acetal-PEG-PLys(SH) was obtained under treatment of DTT for PEG-PLys(PDP).

Synthesis of cRGD-PEG-PLys(SH)

The cyclo(RGDfK(C-ε-Acp)) (cRGD) peptide ligand was attached onto the α-terminal of acetal-PEG-PLys(SH) through formation of a thiazolidine ring between the N-terminal cysteine of the cRGD peptide and the aldehyde group from acetal-PEG-PLys following incubation at acidic pH (pH = 2). In brief, acetal-PEG-PLys(SH) was dissolved in 10 mM HEPES buffer (pH 7.4) and dialyzed against 0.01 N HCl (pH 2.0) to yield aldehyde from the acetal group, followed

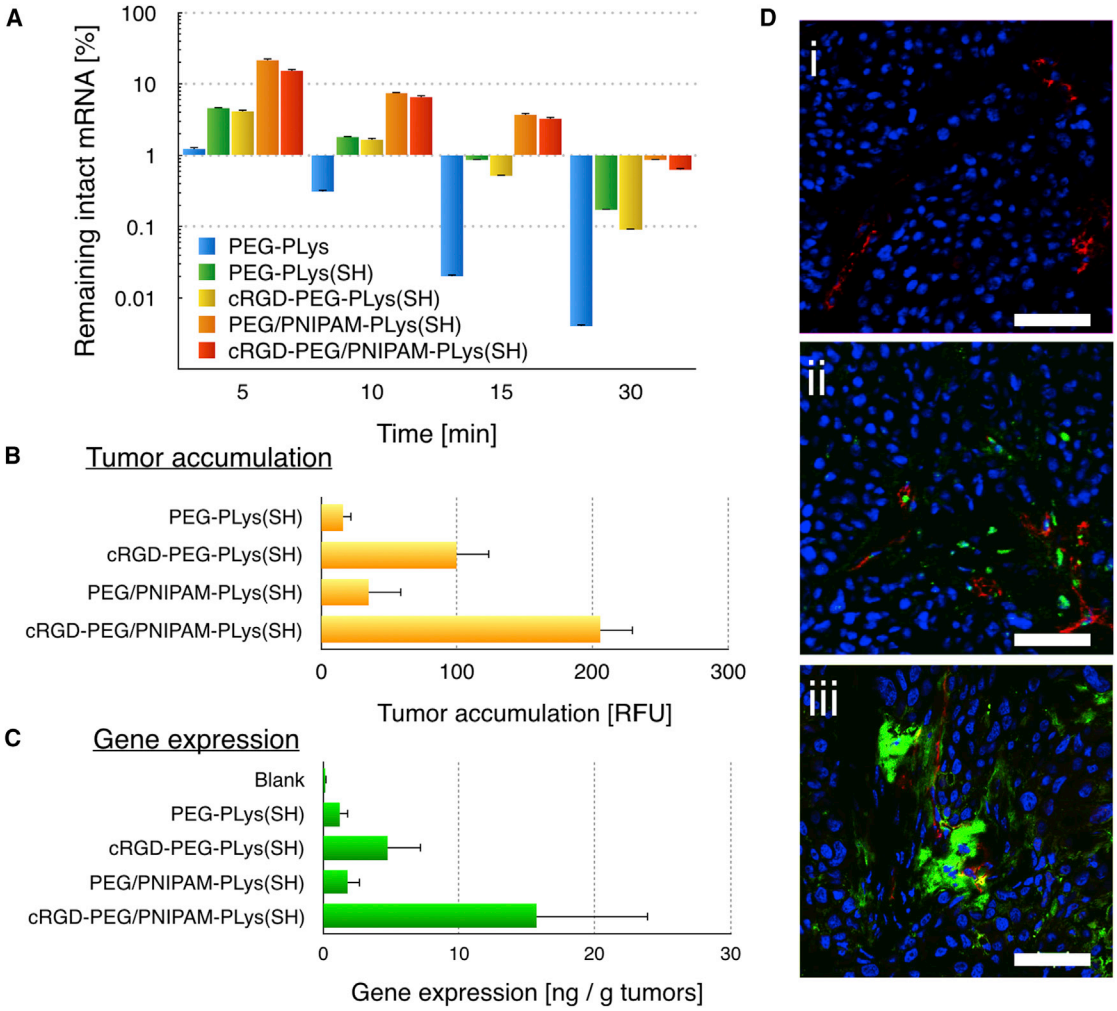

Figure 5. In Vivo Performances of the Diverse Polymeric Formulations

(A) Pharmacokinetics of mRNA within varying polymeric nanoformulations post intravenous administration (ANOVA analysis was conducted on all the groups; $p < 0.01$). (B) Tumor accumulation efficiency of diverse polymeric formulations at 24 hr post intravenous administration is shown (ANOVA analysis was conducted on all the groups; $p < 0.05$). (C) Quantification of mRNA expression (GFP) in tumors by diverse polymeric formulations at 48 hr post intravenous administration is shown (ANOVA analysis was conducted on all the groups; $p < 0.05$). (D) Representative mRNA expression in tumors at 48 hr post intravenous administration is shown; (i): PBS; (ii): PEG/PNIPAM-PLys(SH); (iii): cRGD-PEG-PNIPAM-PLys(SH); scale bar: 200 μm.

by addition of the DTT-pretreated cRGD solution. The reaction was conducted at pH 4.5 by pH adjustment by 0.01 N NaOH. After stirring overnight at 25°C, the polymer solution was dialyzed against HEPES (pH 7.4), followed by distilled water. Eventually, the solution was collected and lyophilized to obtain cRGD-PEG-PLys(SH). The percentage of cRGD conjugation was determined by the peak intensity ratio of benzyl protons (D-phenyl alanine; f: D-Phe; δ = 7.3–7.4 ppm) of the cRGD peptide to the methylene protons of PEG (δ = 3.7 ppm) from the ^{1}H-NMR spectra, and the conjugation ratio of cRGD was calculated to be 95% (Figure S4).

Synthesis of PNIAPM-PLys(SH)

A similar approach to synthesize PEG-PLys(SH) was followed to prepare PNIPAM. In brief, PNIPAM with a terminal functionalized NH_2 group acted as initiator for polymerization of monomer NCA-Lys(TFA), followed by NaOH treatment to remove protective TFA residue. Ultimately, PDP groups were introduced into the side chain of lysine units of the PLys segment of PEG-PLys using the heterobifunctional reagent SPDP.

Preparation of Polymeric Formulations

PEG-PLys and mRNA were separately dissolved in 10 mM HEPES (pH 7.4). Polymeric formulations were simply prepared by fast mixing one-unit volume of the PEG-PLys solution with two-unit volume of mRNA solution at the N/P ratio of 1.5. The N/P ratio is defined as the residual molar ratio of amine (N) groups of PEG-PLys to the phosphate (P) groups of mRNA. On the other hand, for preparation of crosslinked polymeric formulation, block copolymer, such

as PEG-PLys(SH) or mixture of PNIPAM-PLys(SH) and cRGD-PLys(SH), was dissolved in 100 mM DTT containing 10 mM HEPES (pH 7.4) and incubated for 4 hr at RT to cleave any undesired preliminary formation of disulfide bonds. Polymeric formulations were prepared at the N/P ratio of 1.5 by fast mixing the pre-DTT-treated polymer solution with mRNA solution. After 1 hr incubation at 4°C, polymeric nanoformulations were transferred to dialysis cassettes and dialyzed against 0.5% DMSO containing HEPES for 12 hr, followed by additional dialysis against only HEPES at 4°C for 24 hr to remove DTT and DMSO from the polymeric formulation solutions. Note that DMSO was added to the dialysis buffer as an oxidizing agent with the aim of facilitating the formation of disulfide crosslinking between a PLys(SH) segment of the polymers. The polymeric nanoformulation solutions were recovered from dialysis cassettes, and the mRNA concentration in the solutions was measured by NanoDrop ND-1000 (NanoDrop Technologies).

Determination of the Thermoresponsivity of the Polymeric Formulation by ^{1}H-NMR

The thermoresponsivity of PEG/PNIPAM-PLys(SH) was investigated by ^{1}H-NMR. The ratio of peak area derived from the protons from PEG or that of PNIPAM was measured as a function of incubation temperature in D_2O, and the result was normalized against the ratio at 20°C. The temperature was increased from 20°C to 45°C in a stepwise manner.

Fluid AFM Characterization

AFM imaging of the polymeric nanoformulation was performed using a MMAFM, Nanoscope IIIa (Veeco) in tapping mode with standard silicon probes. Note that the polymeric nanoformulation of PEG/PNIPAM-PLys(SH)/mRNA was prepared at 25°C. AFM measurement was conducted onto a thermal incubator preset at 25°C or 37°C. Imaging was conducted under aqueous conditions on a highly orientated pyrolytic graphite substrate. The obtained images were processed with flattening treatment with the aim of removing the background slope of the substrate surface.

TEM Characterization

The morphology of mRNA polymeric formulations was observed using the H-7000 TEM machine (Hitachi) operated at an acceleration voltage of 75 kV. In brief, copper TEM grids (Nisshin EM) possessing protective carbon-coated collodion membrane were glow discharged using an Eiko IB-3 ion coater (Eiko Engineering) for surface hydrophilizing treatment. Furthermore, the surface-hydrophilized grids were immersed into uranyl acetate (UA) (2% w/v)-treated polymeric formulation solutions (staining). The sample-deposited grids were blotted onto the filter paper to remove excess solution, followed by thermal block incubation at predefined temperature (at 25°C or 37°C) for air drying for 30 min. The grids were transferred to the TEM observation.

DLS

The hydrodynamic diameter and PDI of polymeric formulations were measured by DLS using a Zetasizer Nanoseries instrument (Malvern Instruments). The measurement was performed three times at a detection angle of 173° and a temperature of 25°C or further extended incubation at 37°C. The rate of decay in the photon correlation function was analyzed according to a cumulant method, and the corresponding diameter was calculated using the Stokes-Einstein equation.

Zeta Potential Measurement

The zeta potential of the polymeric nanoformulations was also measured by Nano ZS (ZEN3600; Malvern Instruments). The polymeric nanoformulation solution was injected into folded capillary cells (Malvern Instruments). The zeta potential was determined from the laser Doppler electrophoresis using the Zetasizer nanoseries (Malvern Instruments). From the obtained electrophoretic mobility, the zeta potential was calculated by using the Smoluchowski equation: $\varsigma = 4\pi\eta\nu/\varepsilon$, in which η is the electrophoretic mobility, ν is the viscosity of the solvent, and ε is the dielectric constant of the solvent. The results are expressed as the average of three experiments.

SyBr Green II Assay

Dextran sulfate was dissolved in 10 mM HEPES (pH 7.4) buffer as stock solution (5 mg/mL). Then, diverse polymeric formulation solutions (18 μL) were fused with aliquot of dextran sulfate stock solution at varying concentrations. The samples were allowed for 1 hr polyion exchange reaction at room temperature, followed supplement with SyBr Green II for reaction for 3 hr. The fluorescence intensity of SyBr Green II was measured by Nanodrop (ex: 479 nm; em: 520 nm).

Quantification of mRNA after Serum Incubation by Quantitative Real-Time PCR

Solutions of polymeric nanoformulations containing *Luc* mRNA at an mRNA concentration of 50 mg/mL were incubated in 50% fetal bovine serum for 60 min at 37°C. After sequential treatment with trypsin at 37°C and dextran sulfate and DTT at 4°C, mRNA purification was conducted with the RNeasy Mini Preparation Kit (QIAGEN). The purified product was transferred for quantitative real-time PCR using an ABI Prism 7500 Detector (Applied Biosystems), where a primer pair for *Luc* (forward: TGCAAAAGATCCTCAACGTG; reverse: AATGGGAAGTCACGAAGGTG) was used.

Cellular Uptake

U87 cells were seeded onto 6-well culture plates (50,000 cells/well) with 2,000 μL of DMEM containing 10% FBS and 1% antibiotics (penicillin and streptomycin) and incubated in a humidified atmosphere supplemented with 5% CO_2 at 37°C. After 24 hr incubation, the medium was replaced with fresh medium. The cells were treated with polymeric formulation solutions (1 μg of Cy5-labeled mRNA/well) and followed by incubation. After another 24 hr, the medium was discarded. The cells were washed three times with ice cold PBS to remove extracellular fluorescence. The cells were detached by trypsin-EDTA treatment and harvested from the cell culture plate as suspension in 1 mL ice cold PBS. The cellular uptake efficiency was measured by a BD LSR II flow cytometer equipped with FACS-Diva software (BD Biosciences). The obtained data were expressed

as the mean fluorescence intensity from three independent samples (n = 3).

Cytotoxicity

U87 cells were plated onto 24-well culture dishes (20,000 cells/well) in 400 μL DMEM containing 10% FBS and 1% antibiotics (penicillin and streptomycin) and incubated in a humidified atmosphere with 5% CO_2 at 37°C. After 24 hr incubation, the medium was replaced with 400 μL fresh medium, followed by the addition of polymeric formulation solutions containing 0.5 μg mRNA. After 24 hr incubation, the medium was replaced with fresh medium, followed by another 24-hr incubation. The cells were washed three times with ice cold PBS, followed by the addition of 200 μL of fresh medium. Cell viability was assessed on the basis of 2-(2-methoxy-4-nitrophenyl)-3-(4-nitrophenyl)-5-(2,4-disulfophenyl)-*2H*-tetrazolium (WST-8) reduction to WST-8 formazan by the dehydrogenase activity of viable cells using the Cell Counting Kit-8 (CCK-8) (Dojindo) according to manufacturer's instructions.

Transfection Efficiency

U87 cells were seeded onto 24-well culture plates (20,000 cells/well) with 400 μL of DMEM containing 10% FBS and 1% antibiotics (penicillin and streptomycin) and incubated for 24 hr in a humidified atmosphere supplemented with 5% CO_2 at 37°C. After exchanging the medium with a fresh one, 1 μg of *Luc* mRNA containing polymeric formulation solutions was added to each well. After 24 hr incubation, the medium was exchanged with 400 μL of fresh medium, followed by another 24-hr incubation. The cells were washed three times with 400 μL of ice cold PBS and lysed by 150 μL of cell culture lysis buffer at 37°C for 15 min. Immediately, 20 μL of the cell lysate was transferred to a 96-well luminometry plate, followed by the addition of 100 μL of Luciferase Assay Reagent (Promega) to each well, and allowed to react for 15 min. The *Luc* expression was then measured for 10 s from the photoluminescence intensity using Mithras LB 940 (Berthold Technologies). The amount of total protein in the cell lysate was quantified using the Micro BCA Protein Assay Kit (Pierce), and the obtained *Luc* activity was normalized against the corresponding amount of total protein in the cell lysates. The data were expressed as relative light units (RLUs) per mg of protein (RLU/mg protein) (n = 6).

mRNA Survival in Blood Circulation

BALB/C mice (5 weeks; female) were purchased from Charles River Laboratories. Solutions of polymeric formulations containing *Luc* mRNA at an mRNA concentration of 50 mg/mL were administered into the mice via intravenous injection. Blood was collected after submandibular bleeding at varying time points. The blood samples were lysed with equal volume of Passive Lysis Buffer (Promega). After sequential treatment with trypsin at 37°C and dextran sulfate and DTT at 4°C, mRNA purification was conducted with the RNeasy Mini Preparation Kit (QIAGEN). The purified product was transferred for quantitative real-time PCR using an ABI Prism 7500 Detector (Applied Biosystems), where a primer pair for *Luc* (forward: TGCAAAAGATCCTCAACGTG; reverse: AATGGGAAGTCACGA AGGTG) was used for PCR.

Tumor Accumulation

BALB/c nude mice were inoculated subcutaneously with U87 cells (10^7 cells in 100 mL of PBS). Tumors were allowed to grow for 3 weeks (tumor size was approximately 300 mm^3). Mice were randomly selected for two cohorts (n = 5). Solution of polymeric formulations (0.2 mL) prepared from *Luc* mRNA was intravenously injected into the blood stream through the tail vein to quantify the tumor accumulation efficiency. Mice were sacrificed 24 hr after injection. The tumor tissue was excised. The lysed solution of tumor tissue was transferred to quantitative real-time PCR measurement.

mRNA Expression in Tumors

Polymeric formulation containing GFP (10 μg in 200 μL of 10 mM HEPES containing 150 mM NaCl) was intravenously injected once into the tumor-bearing mice via the tail vein. The mice were sacrificed after 48 hr of injection, and xenografted tumors were excised, placed into tissue-Tek-OCT, frozen at −80°C for 2 days, and sectioned into 10-μm-thick slices with a rotary microtome maintained in a cryostat at −20°C, followed by transfer onto a microscopic slide. Vascular endothelial cells (VECs) of the tumor vasculature were immunofluorescent stained by rat monoclonal antibody against mouse PECAM-1, followed by incubation with Alexa-Fluor-647-conjugated goat anti-rat immunoglobulin G (IgG) (H + L) secondary antibody (A21247) (Invitrogen). The nuclei were fluorescent stained with Hoechst 33342 (H3570) (Invitrogen). The immunofluorescent-stained tumor sections were analyzed for fluorescence using a CLSM, LSM 780 (Carl Zeiss). The GFP expression was quantified by quantification of florescence intensity of homogenized tissue by in vivo imaging system (IVIS), where the result was normalized against the protein concentration of homogenized tissue.

Statistical Analysis

The p values were determined by the Student's t test using a two-tailed distribution and two-sample un-equal variance with the t test function of Microsoft Excel for statistical analysis for two samples. ANOVA was conducted for statistical analysis for more than two groups. The p values of less than 0.05 were considered statistically significant.

SUPPLEMENTAL INFORMATION

Supplemental Information includes Supplemental Materials and Methods, eight figures, and three schemes and can be found with this article online at http://dx.doi.org/10.1016/j.ymthe.2016.10.006.

AUTHOR CONTRIBUTIONS

Conceptualization, Q.C. and R.Q.; Methodology, Q.C., R.Q., X.Y., and H.X.; Investigation, Q.C., X.C., and W.D.; Writing – Original Draft, Q.C. and X.C.; Writing – Review & Editing, Q.C. and W.D.; Funding Acquisition, W.D.; Resource, Q.C. and W.D.; Supervision, Q.C., X.C., and W.D.

ACKNOWLEDGMENTS

This work was financially supported by the National Natural Science Foundation of China (grant no. 61535010) and the Science and Technology Department of Suzhou City (no. ZXY201434).

REFERENCES

1. Kay, M.A. (2011). State-of-the-art gene-based therapies: the road ahead. Nat. Rev. Genet. *12*, 316–328.
2. Mingozzi, F., and High, K.A. (2011). Therapeutic *in vivo* gene transfer for genetic disease using AAV: progress and challenges. Nat. Rev. Genet. *12*, 341–355.
3. Naldini, L. (2011). Ex vivo gene transfer and correction for cell-based therapies. Nat. Rev. Genet. *12*, 301–315.
4. Lee, Y., and Kataoka, K. (2012). Delivery of nucleic acid drugs. Adv. Polym. Sci. *249*, 95–134.
5. Brandén, L.J., Mohamed, A.J., and Smith, C.I. (1999). A peptide nucleic acid-nuclear localization signal fusion that mediates nuclear transport of DNA. Nat. Biotechnol. *17*, 784–787.
6. Ziemienowicz, A., Görlich, D., Lanka, E., Hohn, B., and Rossi, L. (1999). Import of DNA into mammalian nuclei by proteins originating from a plant pathogenic bacterium. Proc. Natl. Acad. Sci. USA *96*, 3729–3733.
7. Subramanian, A., Ranganathan, P., and Diamond, S.L. (1999). Nuclear targeting peptide scaffolds for lipofection of nondividing mammalian cells. Nat. Biotechnol. *17*, 873–877.
8. Ponsaerts, P., Van Tendeloo, V.F., and Berneman, Z.N. (2003). Cancer immunotherapy using RNA-loaded dendritic cells. Clin. Exp. Immunol. *134*, 378–384.
9. Dirisala, A., Osada, K., Chen, Q., Tockary, T.A., Machitani, K., Osawa, S., Liu, X., Ishii, T., Miyata, K., Oba, M., et al. (2014). Optimized rod length of polyplex micelles for maximizing transfection efficiency and their performance in systemic gene therapy against stroma-rich pancreatic tumors. Biomaterials *35*, 5359–5368.
10. Kakizawa, Y., and Kataoka, K. (2002). Block copolymer micelles for delivery of gene and related compounds. Adv. Drug Deliv. Rev. *54*, 203–222.
11. Veronese, F.M., and Pasut, G. (2005). PEGylation, successful approach to drug delivery. Drug Discov. Today *10*, 1451–1458.
12. Tockary, T.A., Osada, K., Chen, Q., Machitani, K., Dirisala, A., Uchida, S., Nomoto, T., Toh, K., Matsumoto, Y., Itaka, K., et al. (2013). Tethered PEG crowdedness determining shape and blood circulation profile of polyplex micelle gene carriers. Macromolecules *46*, 6585–6592.
13. Ge, Z., Chen, Q., Osada, K., Liu, X., Tockary, T.A., Uchida, S., Dirisala, A., Ishii, T., Nomoto, T., Toh, K., et al. (2014). Targeted gene delivery by polyplex micelles with crowded PEG palisade and cRGD moiety for systemic treatment of pancreatic tumors. Biomaterials *35*, 3416–3426.
14. Ward, M.A., and Georgiou, T.K. (2011). Thermoresponsive polymers for biomedical applications. Polymers *3*, 1215–1242.
15. Tuma, R.S., Beaudet, M.P., Jin, X., Jones, L.J., Cheung, C.Y., Yue, S., and Singer, V.L. (1999). Characterization of SYBR Gold nucleic acid gel stain: a dye optimized for use with 300-nm ultraviolet transilluminators. Anal. Biochem. *268*, 278–288.
16. Zuckerman, J.E., Choi, C.H.J., Han, H., and Davis, M.E. (2012). Polycation-siRNA nanoparticles can disassemble at the kidney glomerular basement membrane. Proc. Natl. Acad. Sci. USA *109*, 3137–3142.
17. Takayama, S., Ishii, S., Ikeda, T., Masamura, S., Doi, M., and Kitajima, M. (2005). The relationship between bone metastasis from human breast cancer and integrin alpha(v)beta3 expression. Anticancer Res. *25* (1A), 79–83.
18. Furger, K.A., Allan, A.L., Wilson, S.M., Hota, C., Vantyghem, S.A., Postenka, C.O., Al-Katib, W., Chambers, A.F., and Tuck, A.B. (2003). Beta(3) integrin expression increases breast carcinoma cell responsiveness to the malignancy-enhancing effects of osteopontin. Mol. Cancer Res. *1*, 810–819.
19. Vellon, L., Menendez, J.A., Liu, H., and Lupu, R. (2007). Up-regulation of alphavbeta3 integrin expression is a novel molecular response to chemotherapy-induced cell damage in a heregulin-dependent manner. Differentiation *75*, 819–830.
20. Brooks, P.C., Clark, R.A., and Cheresh, D.A. (1994). Requirement of vascular integrin alpha v beta 3 for angiogenesis. Science *264*, 569–571.
21. Srivatsan, A., Ethirajan, M., Pandey, S.K., Dubey, S., Zheng, X., Liu, T.H., Shibata, M., Missert, J., Morgan, J., and Pandey, R.K. (2011). Conjugation of cRGD peptide to chlorophyll a based photosensitizer (HPPH) alters its pharmacokinetics with enhanced tumor-imaging and photosensitizing (PDT) efficacy. Mol. Pharm. *8*, 1186–1197.
22. Christie, R.J., Matsumoto, Y., Miyata, K., Nomoto, T., Fukushima, S., Osada, K., Halnaut, J., Pittella, F., Kim, H.J., Nishiyama, N., and Kataoka, K. (2012). Targeted polymeric micelles for siRNA treatment of experimental cancer by intravenous injection. ACS Nano *6*, 5174–5189.

YMTHE, Volume *25*

Supplemental Information

A Targeted and Stable Polymeric Nanoformulation Enhances Systemic Delivery of mRNA to Tumors

Qixian Chen, Ruogu Qi, Xiyi Chen, Xi Yang, Sudong Wu, Haihua Xiao, and Wenfei Dong

Supplemental data items:

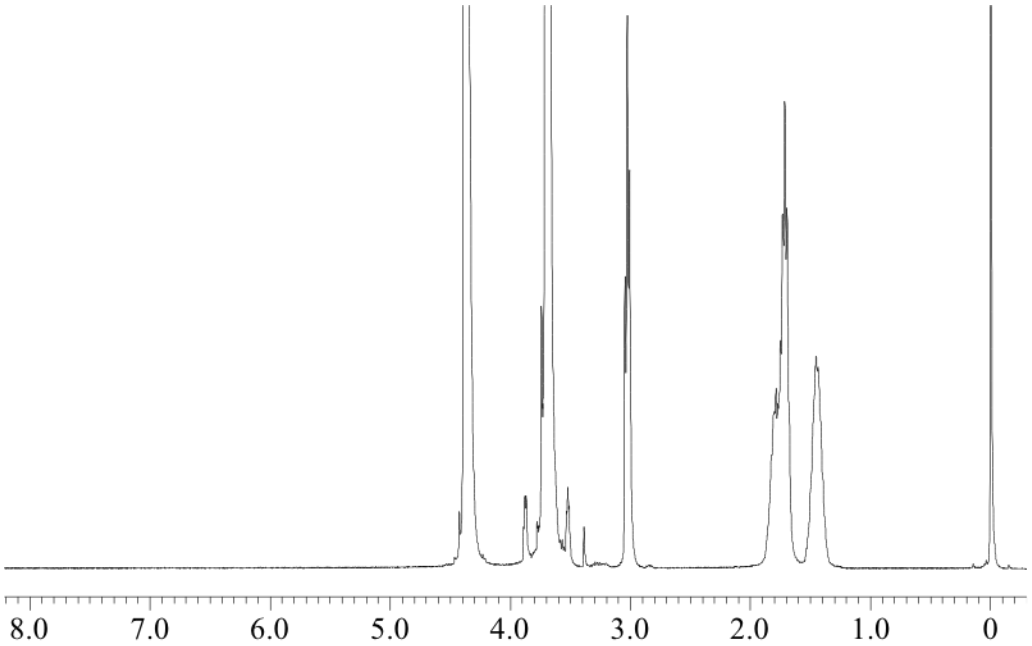

Figure S1 ^{1}H-NMR spectra of PEG-PLys in D_2O at 80 °C.

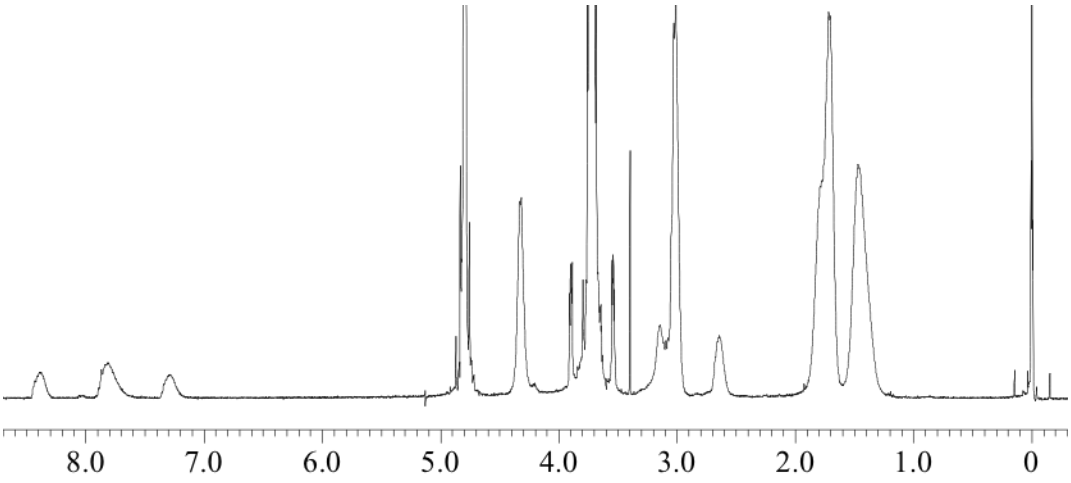

Figure S2 ^{1}H-NMR spectra of PEG-PLys(PDP) in D_2O at 80 °C.

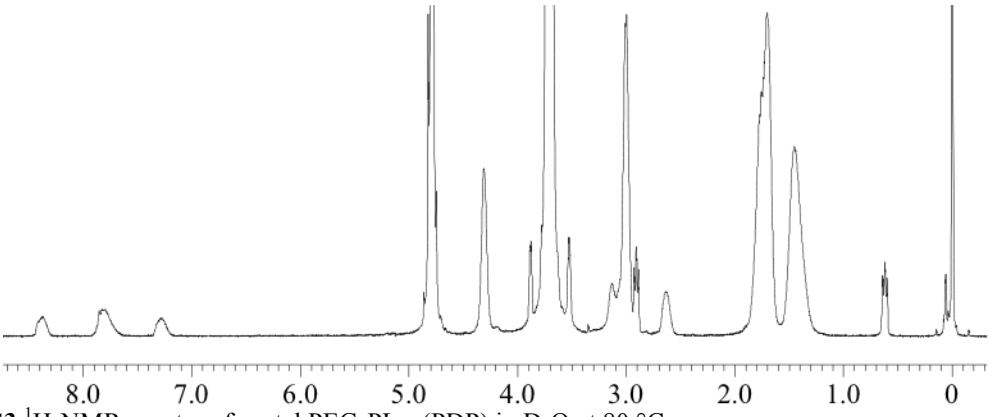

Figure S3 ^{1}H-NMR spectra of acetal PEG-PLys(PDP) in D_2O at 80 °C.

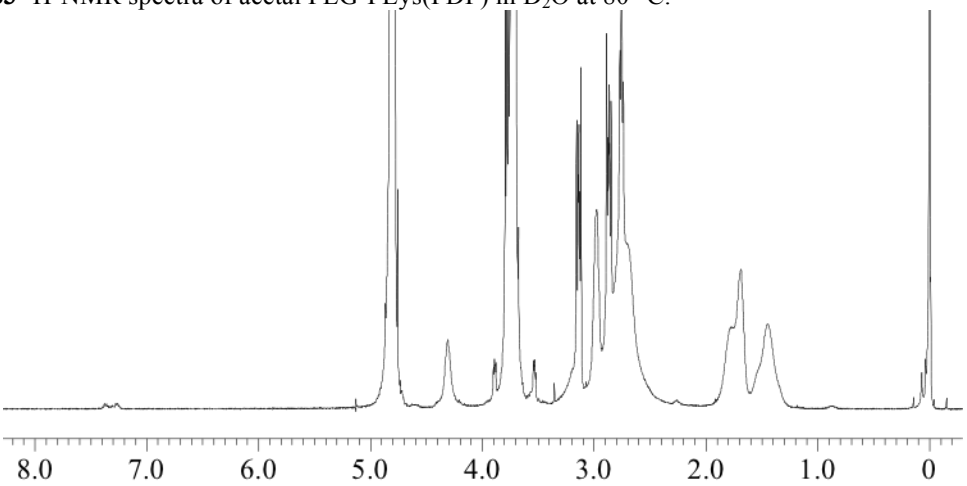

Figure S4 ^{1}H-NMR spectra of cRGD-PEG-PLys(PDP) in D_2O at 80 °C.

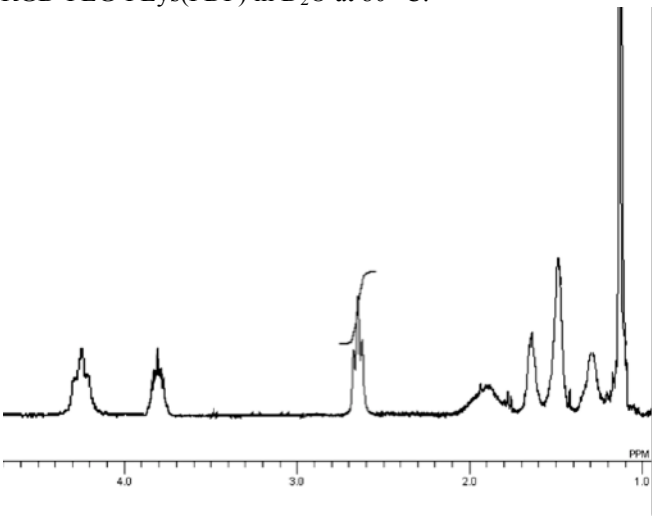

Figure S5 ^{1}H-NMR spectra of PNIPAM-PLys(PDP) in D_2O at 20 °C.

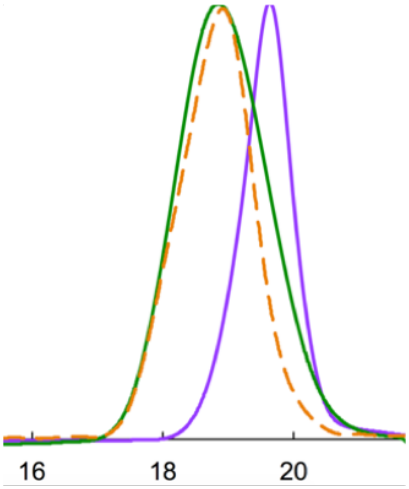

Figure S6 GPC trace of PEG-PLys (orange), cRGD-PEG-PLys(SH) (green) and PNIPAM-PLys(SH) (purple).

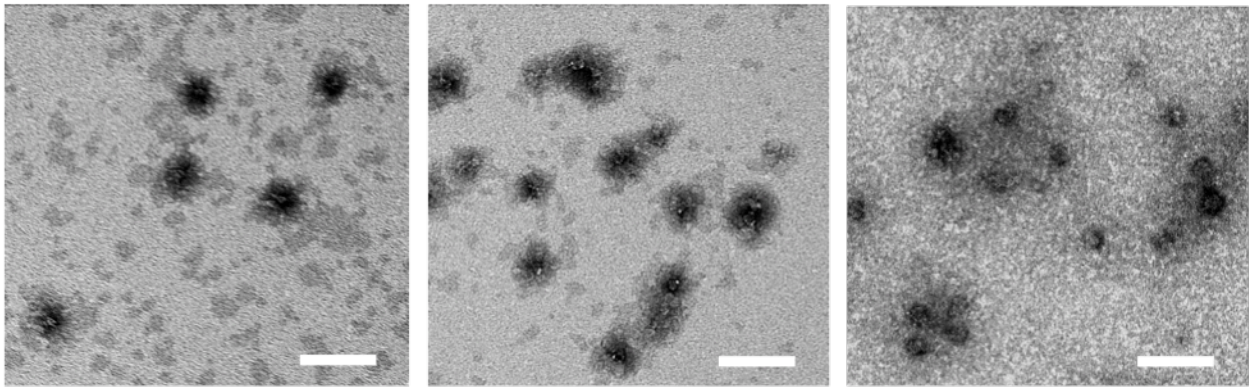

Figure S7 TEM morphology of diverse polymeric formulations. Polymeric formulation of PEG-PLys(SH) (left), PEG/PNIPAM-PLys(SH) at 25 °C and PEG/PNIPAM-PLys(SH) at 37 °C. Scale bar: 200 nm.

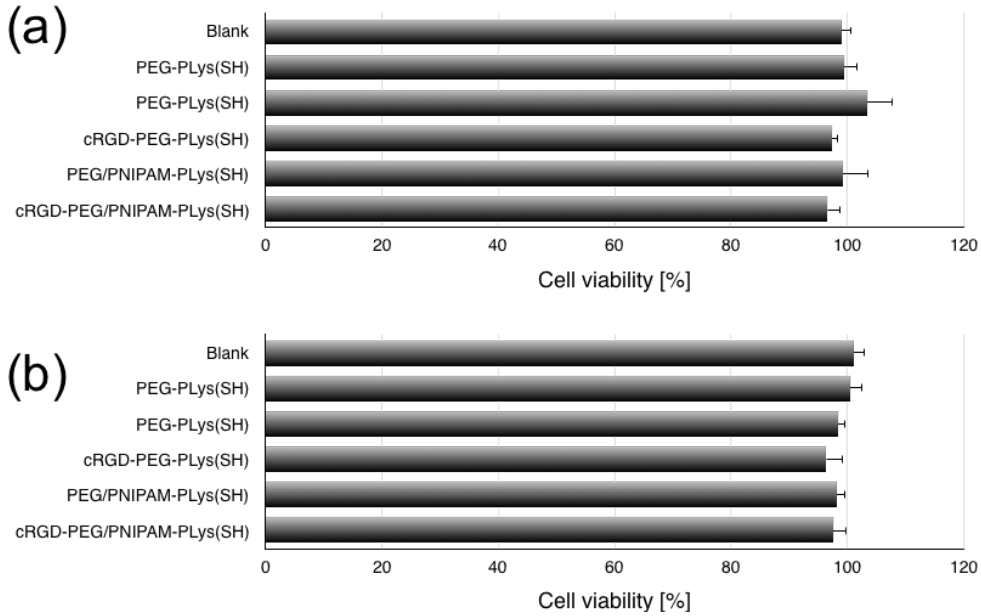

Figure S8 Cell viability of U87 cells and HUVECs in presence of diverse polymeric formulations.

Supplemental Methods:

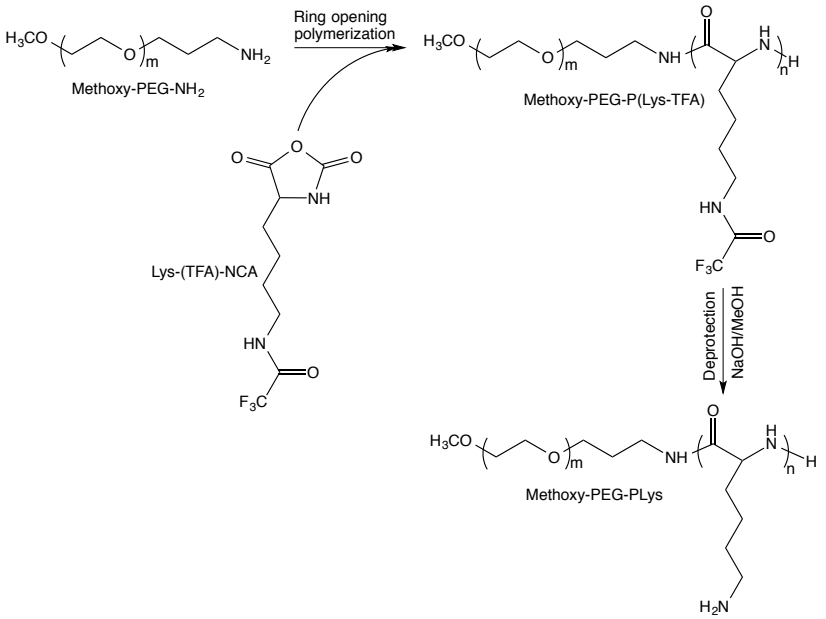

Scheme S1 Synthetic scheme to prepare block copolymer PEG-PLys

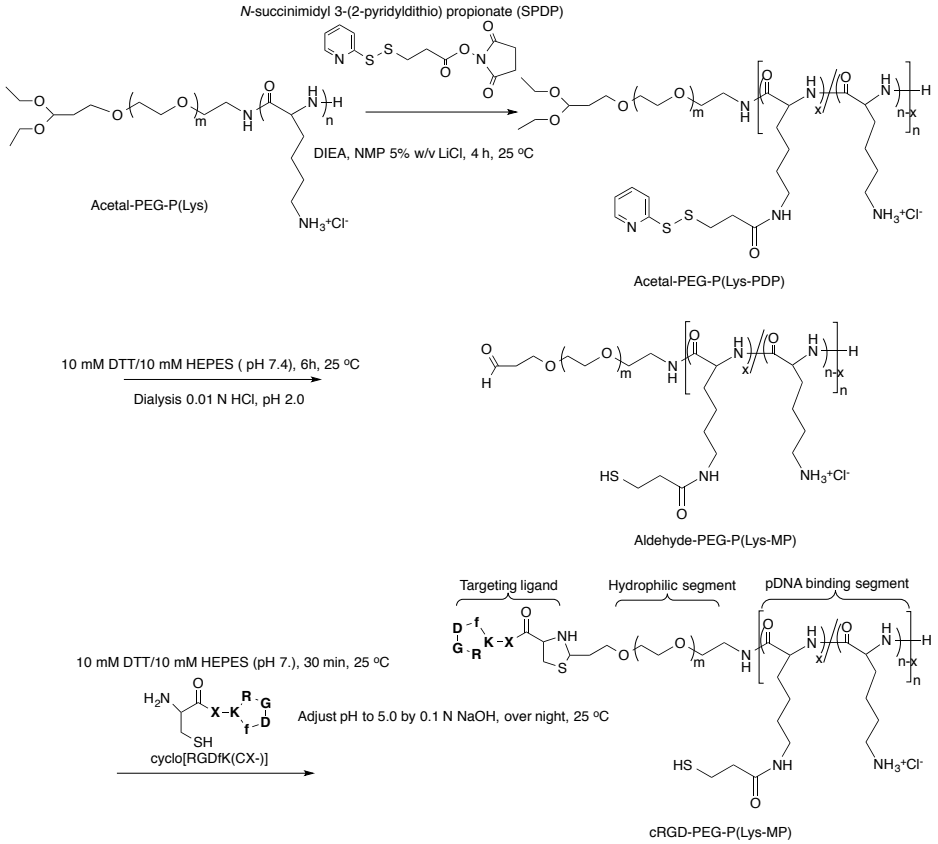

Scheme S2 Synthetic scheme to prepare block copolymer cRGD-PEG-PLys(SH).

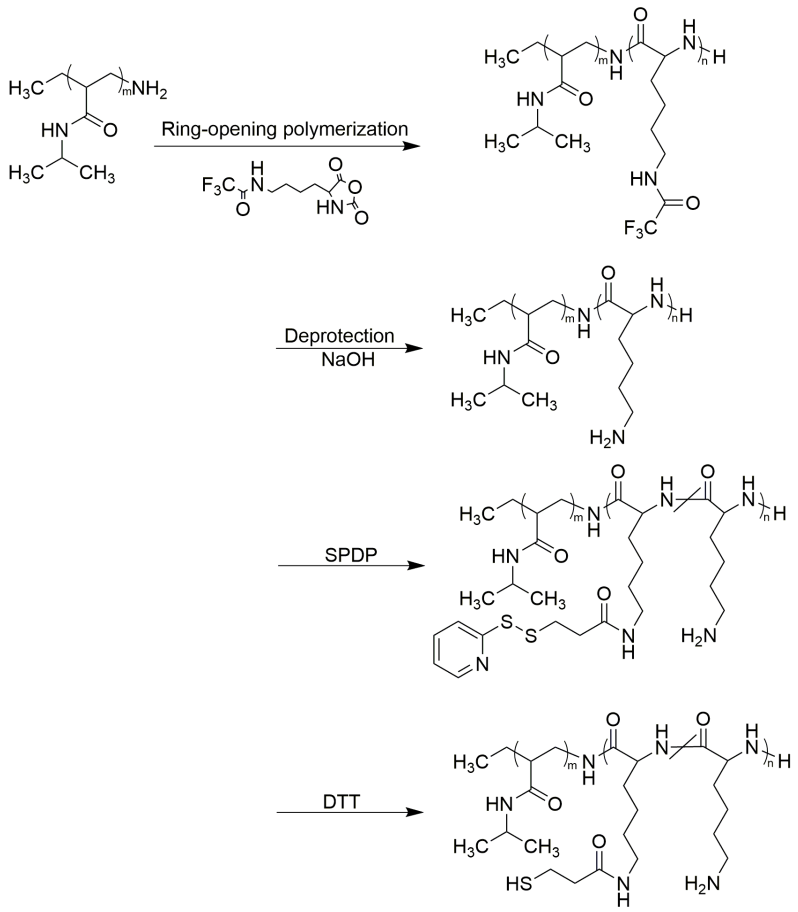

Scheme S3 Synthetic scheme to prepare block copolymer PNIPAM-PLys(SH)

Transmission electron microscopy (TEM) characterization

The morphology of polymeric formulations was observed using the H-7000 TEM machine (Hitachi Ltd., Tokyo, Japan) operated at an acceleration voltage of 75 kV. In brief, copper TEM grids (Nisshin EM Corp., Japan) containing carbon-coated collodion membrane were glow-discharged for 30 s using an Eiko IB-3 ion coater (Eiko Engineering Co. Ltd., Japan) for hydrophilization. The hydrophilized grids were immersed into uranyl acetate (UA) (2% w/v)-treated PM solutions for 30 s to achieve effective staining. The sample-deposited grids were blotted onto the filter paper to remove excess solution, followed by air-drying for 30 min. The grids were transferred to the TEM observation.

Cytotoxicity

U87 cells [or Human Umbilical Vein Endothelial Cells (HUVECs)] were plated onto 24-well culture dishes (20,000 cells/well) (or collagen I coated 24-well culture dishes for HUVECs) in 400 µl DMEM containing 10% FBS and 1% antibiotics (penicillin and streptomycin) (or HUVEC-Umbilical Vein Endo, EGM-2, amp AMP for HUVECs, Lonza, Basel, Switzerland) and incubated in a humidified atmosphere with 5% CO_2 at 37 °C. After 24 h of incubation, the medium was replaced with 400 µl of fresh medium, followed by the addition of polymeric formulation solutions equivalent to 0.5 µg of pDNA/well. After 24 h incubation, the medium was replaced with fresh medium, followed by another 24 h of incubation. The cells were washed three times with ice-cold PBS, followed by the addition of 200 µl of fresh medium. Cell viability was assessed on the basis of 2-(2-methoxy-4-nitrophenyl)-3-(4-nitrophenyl)-5-(2,4-disulfophenyl)-*2H*-tetrazolium (WST-8) reduction to WST-8 formazan by the dehydrogenase

activity of viable cells using the Cell Counting Kit-8 (CCK-8) (Dojindo, Kumamoto, Japan) according to manufacturer's instructions. In brief, 20 µl of the CCK-8 reagent was added to each well and allowed to develop orange-colored WST-8 formazan for 2 h. The UV absorbance of WST-8 formazan in each well was quantified at 450 nm using a microplate reader (Model 680, Bio-Rad, UK). The cell toxicity was expressed as the percentage of cell viability normalized against the control cells treated with 10 mM HEPES (pH 7.4) (n = 4).